Int. J. Electrochem. Sci., 11 **(2016)** 1928 - 1937

International Journal of
ELECTROCHEMICAL
SCIENCE
www.electrochemsci.org

A Facile Hydrazine Amperometric Sensor Based on a Glassy Carbon Electrode Modified with Au Nanoparticles-MnO_2 Composites

Mei-Fang Wang,[1,#] *Wei Li,*[1,#] *Ping-Jing Hu,*[1] *Shuang-Shuang He,*[1] *Hong-Mei Yang*[1] *and Xiang-Zi Li*[1,2,*]

[1]Department of Chemistry, WanNan Medical College, Wuhu, 241002, China, Tel: +86 5533932472
[2]School of Chemistry & Chemical Engineering, JiangSu University, ZhengJiang, 212013, China
[#] Equally contribution to this paper.
[*]E-mail: li-xiang-zi@163.com

Received: 27 December 2015 / *Accepted:* 19 January 2016 / *Published:* 1 February 2016

A facile hydrazine sensor based on Au nanoparticles-MnO_2 composite on the glassy carbon electrode (Au/MnO_2/GCE) was directly obtained by electrochemical deposition approach. The prepared modified electrode presented good oxidation peak currents of hydrazine in a wide linear range from 5 μM to 2.0 mM with a correlation coefficient of 0.9998. The sensitivity was 694 μA mM^{-1} cm^{-2} and its detection limit was 1.7 μM (S/N=3).

Keywords: Electrochemistry sensor, Hydrazine, MnO_2 composites

1. INTRODUCTION

With the development of science and technology, there are more and more attentions of electrochemistry analysis in the field of agriculture, industry, medicine and environment [1-2]. Among of them, hydrazine has increasing applications in the field of industrial and agriculture, such as pharmacology, photography chemicals, explosives, fuel cells, corrosion inhibitors, and so on. However, it is well known that hydrazine is also toxic and adverse to human health, especially being embodied in the brain and liver toxicity [3]. So it is very important to accurately detect the concentration of hydrazine in a practical sample, which could protect people from a feasible poisoning. Among various analytical methods for determination of hydrazine, electrochemical techniques have received widely attention due to good efficiency, high sensitivity and low cost [4]. However, in order to minimize overvoltage which can be encountered easily at glassy carbon electrodes in hydrazine detection,

different nanomaterials or composites, such as Au [5-7], Pd [8-9], Ni [10], Ni–B [11], $AuCu_3$ [12], Pd-Au [13], Au/TiO_2 [14], ZnO [15-16], CuO [17-18], Fe_2O_3 [19], $Ni_{1-x}La_x$ [20], PEDOT-Cu_xO [21], Ag-polymer [22-23], PB/SWNTs [24], Co(II)MTpAP [25], Graphene/metal [26-28], have been used to modify the working electrodes. In addition to the above catalytic materials, MnO_2-based nano-composites have been found to be a type of very promising material for detecting hydrazine due to low toxicity, inexpensive, and high electrochemical activity. There are many attempts to enhance the response range and detection limit for hydrazine amperometric sensor by the construction of some complicated nanostructures, such as $Mn_7O_{13}\cdot 5H_2O$/α-MnO_2 nano-hybrid [29], MnO_2/GO composite nanosheets [30], Ni $(OH)_2$–MnO_2 hybrid materials [31], MnO_2/ MWNTs [32], Ag–MnO_2 [33], Cu–MnO_2 [34] and so on. Though some attempts have been carried out to fabricate MnO_2-based modified electrodes, most of them obtained by dropping the mixed suspension of nanomaterials and Nafion onto the surface of the GCE, and which could result in reduction of the conductivity. Moreover, the relation synthesis methods of the MnO_2-based nanomaterials modified onto the electrode surface are not simple. So the development of a facile, fast, direct, sensitive, and stable analytical method for hydrazine is still greatly demanded.

In this work, we present a very useful hydrazine electrochemical sensor based on the nano-Au/MnO_2/GCE by a simple and direct electrodeposition method using CV scanning. The prepared modified electrode shows a good amperometric response for hydrazine due to the synergistic electronic effect of Au nanoparticles and MnO_2 film.

2. EXPERIMENTAL

2.1. Chemicals

$KMnO_4$, NaCl, NH_4Cl, $HAuCl_4$, NaH_2PO_4, Na_2HPO_4, HNO_3, anhydrous ethanol and hydrazine were purchased from Shanghai Sinopharm Chemical Reagent Co., Ltd, China. All chemicals were analytical grade without any further purification. Deionized water (18.2 MΩ cm) used in all experiments was obtained with the Cleaned Ultra pure water system (KNT-III-10).

2.2. Apparatus and electrochemical measurements

The morphologies and microstructures of the as-prepared different modified samples on electrode surfaces were presented by scanning electron microscopy (SEM, Japan, Hitachi S-4800). The chemical compositions of the resulting modified electrodes were also characterized by energy dispersive X-ray spectrometer (EDX, Japan, attached to Hitachi S-4800) and X-ray photoelectron spectroscopy (XPS, American, Thermo ESCALAB 250XI, using Al *Ka* line as the excitation source, $h\nu$ = 1486.6 eV).

All the electrochemical measurements were performed with a CHI 660E electrochemical workstation (Shanghai Chenhua Instrument Company, China). A typical three-electrode system was used with a glassy carbon electrode (GCE, diameter 3.0 mm) as working electrode, a saturated calomel

electrode (SCE) as reference electrode, and a platinum wire as counter electrode. 0.1 M phosphate buffer solutions (PBS) solution with pH 7.0 was used as the electrolyte at room temperature. Electrochemical activities of the samples were recorded by electrochemical impedance spectroscopy (EIS) in a 0.1 M PBS (pH=7.0) quiescent solution in the presence of 2.5×10^{-3} M $[Fe(CN)_6]^{4-/3-}$ and 0.1 M KCl. The frequency range was from 0.1 Hz to 10 kHz, the signal amplitude was 5 mV, and the scan rate was 100 $mV\cdot s^{-1}$.

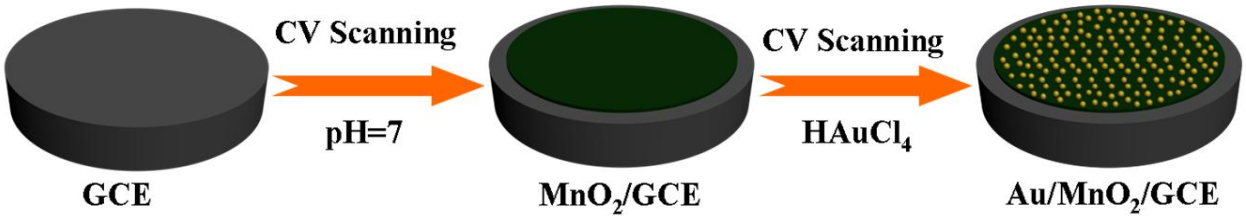

Scheme 1. Schematic illustration of the preparation of Au/MnO_2/ GCE

2.3. Preparation of the Au nanoparticles-MnO_2 modified electrode

The Au/MnO_2 nanocomposites modified electrode was directly fabricated by an easy electrochemical method. The preparation process can be shown in Scheme 1. Firstly, bare GCE was polished successively using 1.0, 0.3 and 0.05 μm alumina slurries, followed by rinsing with 1:1 nitric acid. The electrode was then washed with deionized water and anhydrous ethanol under ultrasound conditions (each for 5 min), and allowed to dry in air at room temperature. MnO_2 films was electrodeposited on a bare GCE surface by cyclic voltammograms (CV) scanning from −0.2 V to +1.2 V at 20 $mV\cdot s^{-1}$ for 6 cycles in 0.1 M PBS solution containing 10 mM $KMnO_4$, 0.5 M NaCl, and 0.5 M NH_4Cl [35]. Subsequently, Au nanoparticles were electrodeposited on the MnO_2 film by CV scanning from −0.2 V to +1.2 V in 5 mM $HAuCl_4$ solution at 100 $mV\cdot s^{-1}$ for 2 cycles, followed by washing with deionized water. As a result, the nano-Au/MnO_2/GCE was obtained, and stored at 4 ˚C in a refrigerator when not in use.

3. RESULTS AND DISCUSSION

3.1. Characterizations of the Au/MnO_2/GCE

As can be seen from Figure 1a, there is a porous and continuous pure MnO_2 film at GCE surface after electrochemical modification. Au nanoparticles were easily obtained by CV scanning with $HAuCl_4$ aqueous solution (Figure 1b), demonstrating the bright and spherical shaped particles with an average diameter of about 25 nm and uniformly spreading on the MnO_2 film. Figure 2a shows the presence of Mn and O, which preliminarily proves the presence of MnO_2 at the electrode surface. The appearances of Au peaks (shown in Figure 2b) further reveal the successful construction of Au/MnO_2/GCE.

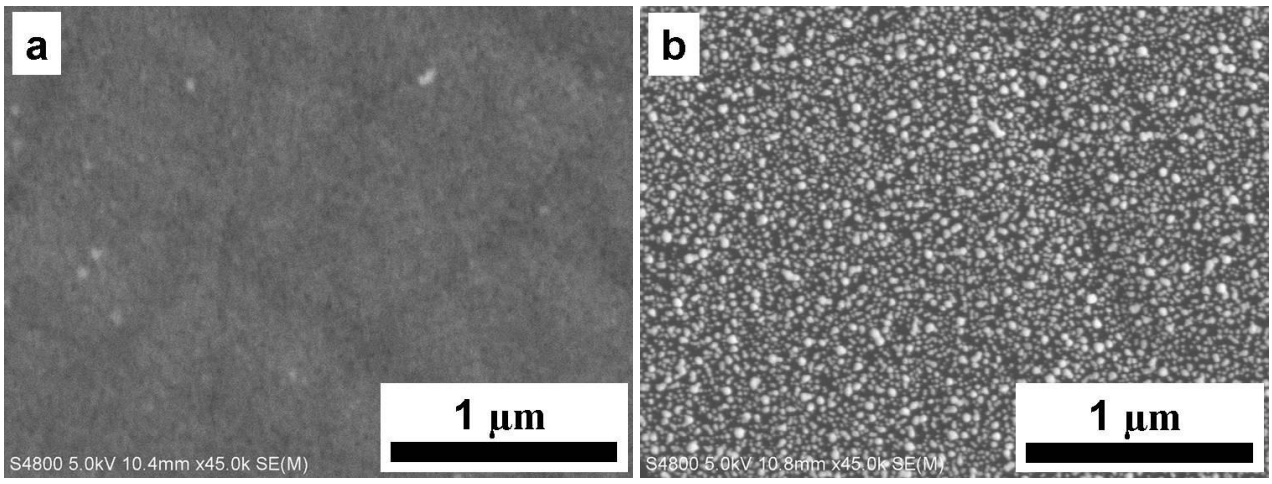

Figure 1. SEM images of MnO_2 (a) and Au-MnO_2 (b) modified on the surface of electrode.

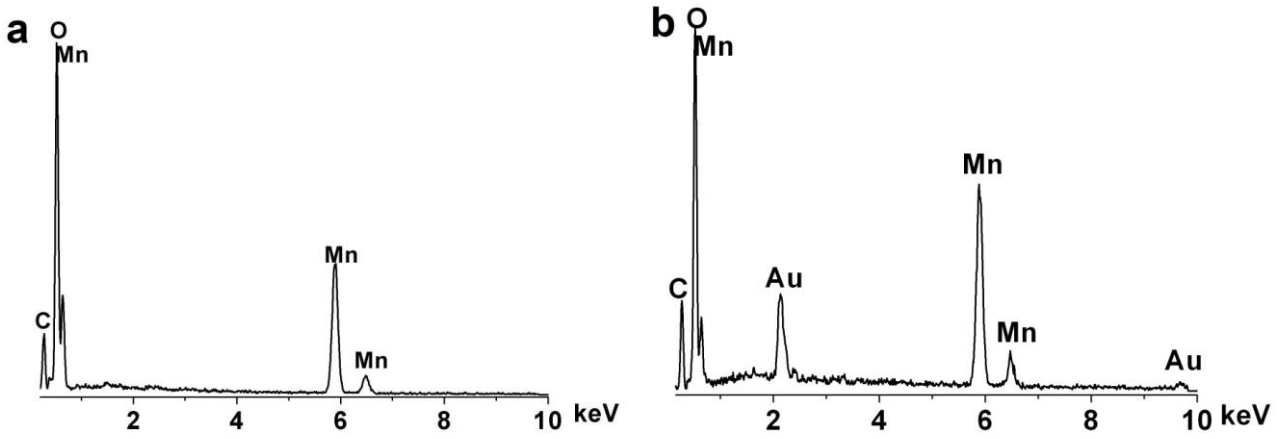

Figure 2. The EDX spectrum of MnO_2 (a) and Au-MnO_2 nanocomposites (b) at the surface of GCE.

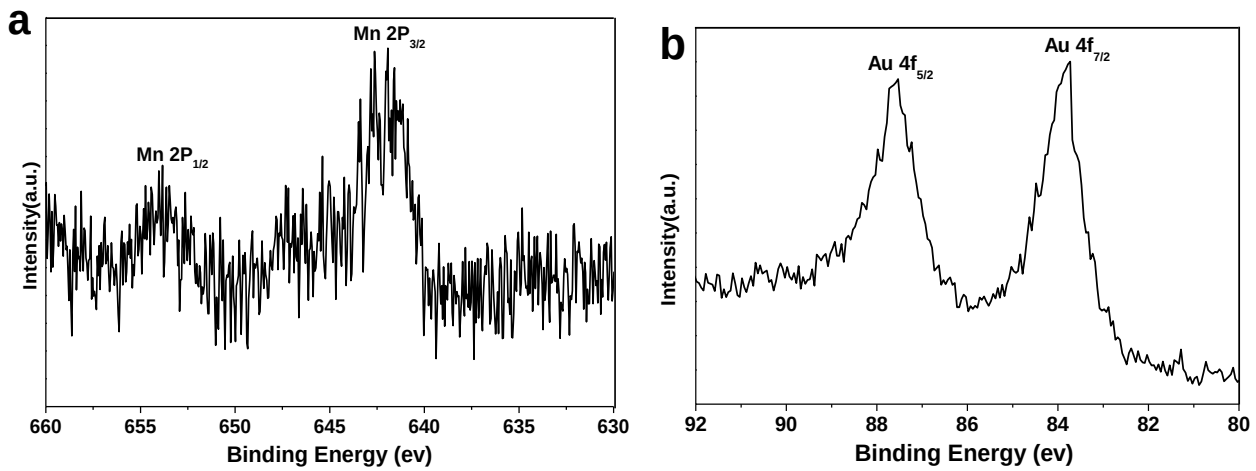

Figure 3. XPS survey spectrum of Mn 2p (a) and Au 4f (b) peaks of the nano-Au/MnO_2 composite.

In order to confirm the formation of MnO_2 not other manganese compounds, XPS was further employed to characterize the valence states and the surface chemical compositions of Au/MnO_2 nanocomposite. However, the prepared product on the GCE surface couldn't be directly characterized with XPS [34], ITO glass was used as a simulative substrate for deposition for Au/MnO_2 nanocomposite under the same electrochemical conditions as the working electrode. As shown in Figure 3a, The Mn 2p XPS spectrum exhibits two typical peaks with binding energy values at 653.8 eV and 642.0 eV respectively [36-37], corresponding to the Mn $2p_{1/2}$ and Mn $2p_{3/2}$ spin-orbit peaks of MnO_2 with a spin-energy separation of 11.8 eV [33]. This result can also be approved by the previous report, in which one binding energy of Mn 2p can vary within the range of 642.0 ± 0.2 eV in the MnO_2-based composites [38]. Figure 3b presents the peaks with binding energy of 83.8 eV and 87.5 eV and peak distance of 3.7 eV, which can be respectively assigned to the binding energies of $4f_{7/2}$ and $4f_{5/2}$ for metallic Au^0 and indicate the presence of gold nanoparticles [39-40], though there maybe some shift of two Au^0 4f peaks toward lower binding energies comparing with Au standard values (84.0 and 87.7 eV) due to the strong metal-support interaction [41]. So the XPS results well indicated that the nano-Au/MnO_2 nanocomposite was electrodeposited successfully onto the surface of GCE.

3.2. Electrochemical properties of the Au/MnO_2/GCE

As can be seen from Figure 4, the Nyquist plots for three electrodes include a semicircular part and a linear part. As is known to all, the semicircle part at the higher frequency presents the electron transfer limited process, and its diameter equals to the electron transfer resistance (R_{et}). There is almost no semicircle part of the GCE, showing a very low R_{et}. However, MnO_2/GCE presents a higher R_{et} of about 443 ohm than the value of bare GCE, indicating a poor electron transfer maybe due to the insulation property of porous MnO_2 film.

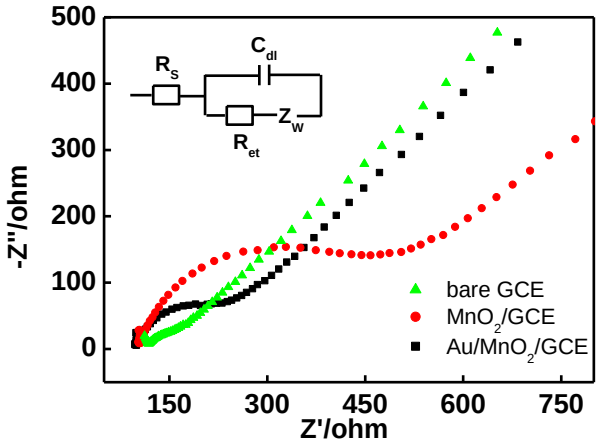

Figure 4. EIS of bare GCE, MnO_2/GCE, Au/MnO_2/GCE in 0.1M PBS (PH 7.0) at a bias potential of 0.2 V.

Contrarily, modification of the MnO_2 film with Au nanoparticles lead to a smaller semicircle and decreased R_{et} (~ 215 ohm), which indicates that high electron transfer took place at the nano-

Au/MnO_2/GCE. The result could show that the continuous distribution and high loading of Au nanoparticles in MnO_2 film can create necessary conduction pathways in promoting the electron transfer on the resultant film electrodes. By the synergistic electron effect between Au and MnO_2, the electrochemical performance of the modified electrode can be dramatically improved [42].

In order to evaluate the eletrocatalytic performance of the nano-Au/MnO_2/GCE, other electrodes (bare GCE, Au/GCE, and MnO_2/GCE) were also examined in pH 7.0 PBS as comparative experiments. In the absence of hydrazine (Figure 5a), there is a pair of very small peaks located at about +0.39 V and +0.69 V for the nano-Au/MnO_2/GCE, which can be assignable to redox process between Mn^{4+} and Mn^{2+} [30]. Furthermore, no obvious redox peaks are found in the potential range of 0 V to +0.8 V at the bare GCE, MnO_2/GCE and Au/GCE. On the contrary, in the presence of 1.0 mM hydrazine, the CV curves of bare GCE, Au/GCE, MnO_2/GCE, and nano-Au/MnO_2/GCE detected in PBS are shown in Figure 5b. As shown from black curve, no obvious redox peaks could be observed at the bare GCE in the potential range of 0 V to +0.8 V. When using the MnO_2/GCE, there is an increasing current response of hydrazine in the oxidation zone and a large overpotential with a very down out peak at about 0.533 V (blue curve) comparing with that of bare GCE. At the Au/GCE electrode, a catalytic oxidation peak at 0.413 V is observed (green curve), which confirms that Au nanoparticles-modified electrode also has eletrocatalytic response for hydrazine [5-7]. However, there is a well-formed sharp catalytic oxidation peak at 0.214 V with a larger peak current (-6.065×10^{-5} A) at nano-Au/MnO_2/GCE (red curve). In contrast, the oxidation peak potentials shift in the negative direction more than 200 mV, which may indicate that the catalytic activity of the electrodes is in the order of nano-Au/MnO_2/GCE > Au/GCE > MnO_2/GCE > bare GCE. Moreover, the increasing current response can be partly attributed to the increase of reversibility of the electron transfer process. The substantial increase in the oxidation peak height at nano-Au/MnO_2/GCE also confirms a faster electron-transfer reaction between electrode and redox probe, which presents better eletrocatalytic performance for hydrazine.

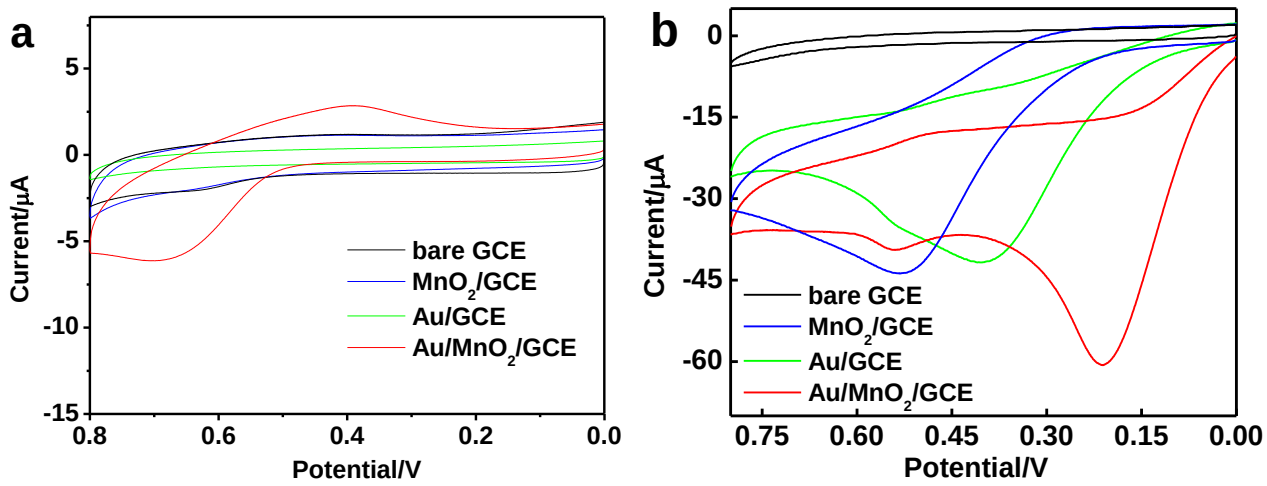

Figure 5. Cyclic voltammograms of bare GCE (black), MnO_2/GCE (blue), Au/GCE (green), and Au/MnO_2/GCE (red) in the absence (a) and presence (b) of 1.0 mM hydrazine in 0.1 M PBS (PH 7.0) at the scan rate of 100 $mV\cdot s^{-1}$.

Differential pulse voltammetry (DPV) was often selected to estimate the detection limit and the linear range for amperometric sensor [43]. Figure 6a displays the DPV response of hydrazine with various concentrations at the obtained nano-Au/MnO_2/GCE carried out in N_2-saturated 0.1 M pH 7.0 PBS (Incr E 0.004 V, amplitude 0.1 V, pulse width 0.05 s, sampling width 0.0167 s, and pulse period 0.5 s). The peak potential is about 0.18 V which is close to that in CV. However, the peak potentials gradually move to positive direction as the concentration of hydrazine successively increased, suggesting that the response of the nano-Au/MnO_2/GCE originate from its high adsorption toward hydrazine.

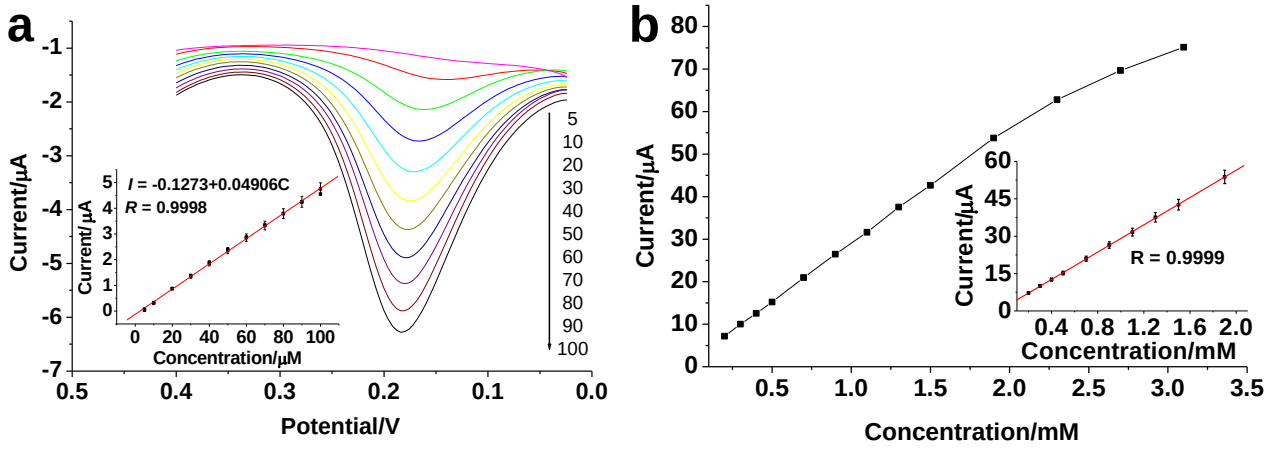

Figure 6. Differential pulse voltammograms of various concentrations of hydrazine at nano-Au/MnO_2/GCE in the presence of 5-100 μM (a) and 0.2-3.1 mM (b) in 0.1 M PBS individually. Inset: the linear dependence of I_{pc} of hydrazine with concentration.

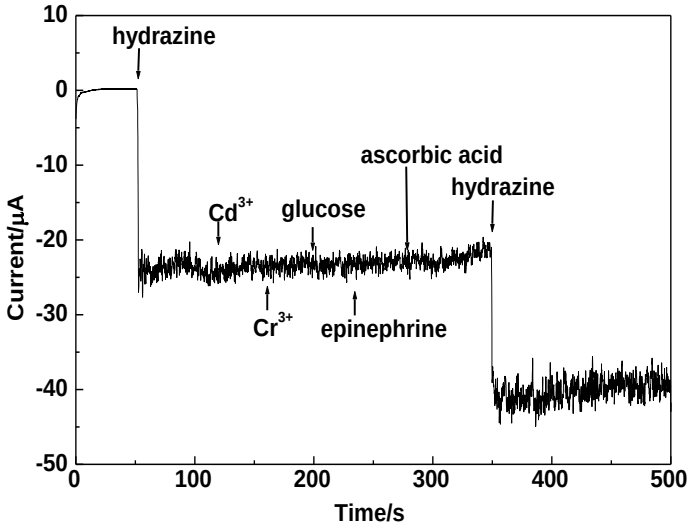

Figure 7. Amperometric response of nano-Au/MnO_2/GCE to 0.3 mM hydrazine and 3.0 mM different interferences.

The I_{pc} of hydrazine increases with the increase in concentration (Figure 6a). As seen in the inset of Figure 6a, the response currents at the nano-Au/MnO_2/GCE are proportional to the concentration of hydrazine in the range of 5-100 μM with a correlation coefficient of 0.999. The regression equation is I (μA) = -0.1273 + 0.04906C, its sensitivity is calculated to be 694 μA mM^{-1} cm^{-2} and detection limit is assessed to be 1.8 μM at a signal/noise ratio of 3. When increasing the range of concentration (0.2 - 3.1 mM, see Figure 6b), the calibration plot for hydrazine determination shows a wide linear response from 0.2 mM to 2.0 mM with a correlation coefficient of 0.9999 (Inset of Figure 6b). It can be clearly seen that the nano-Au/MnO_2 nanocomposites modified electrode is a very simple candidate for an efficient hydrazine sensors.

The selectivity was a very important factor for electrochemical sensors. As the electroactive species, such as heavy metal ions, glucose, epinephrine and ascorbic acid, the hydrazine response of the interfering species was examined at the nano-Au/MnO_2/GCE with the potential of 0.2 V in order to evaluate the selectivity of the as-prepared sensor. As shown in Figure 7, the addition of 0.3 mM hydrazine results in an immediate increase of the oxidation current about 25 μA, while subsequent addition of the high concentration (3 mM) of Cd^{3+}, Cr^{3+}, glucose, epinephrine and ascorbic acid did not show any obvious current response compared to hydrazine. After successive additions of the above interfering species, a further 0.3 mM hydrazine was added into the solution, causing a similar current increase (~20 μA) to that at the first addition. The results can show that the nano-Au/MnO_2/GCE has good selectivity for hydrazine detection.

4. CONCLUSION

In summary, a very simple electrochemical sensor for detection of hydrazine was successfully obtained based on Au/MnO_2 nanocomposites electrodeposited directly on the GCE. The nano-Au/MnO_2/GCE exhibited good electrocatalytic activity to the oxidation of hydrazine, which maybe attribute to the synergistic effect of Au nanoparticles and MnO_2. The hydrazine sensor also showed high sensitivity, excellent selectivity, large detection range and low detection limit, which presented another easy analytical method to detect hydrazine.

ACKNOWLEDGEMENTS

This work was supported by the Foundation of the Natural Science Foundation of Anhui Higher Education Institutions of China (No. KJ2015A158), the Key Projects of the Outstanding Young Talents in Anhui Higher Education Institutions of China (No. gxyqZD2016169), China Postdoctoral Science Foundation Funded Project (No. 2015M581731), Jiangsu Planned Projects for Postdoctoral Research Funds (No. 1501066C), Wuhu Science and Technology Plan of Anhui province of China (No. 2013cxy10), the Doctoral Research Initial Foundation of Wannan Medical College (No. 201221), and the Key Research Culture Funds of Wannan Medical College (No. WK2015Z06).

References

1. A. Shaban, E. Kalman and J. Telegdi, *Electrochim. Acta*, 43 (1998) 159.
2. D. D. Macdonald, *Transient Techniques in Electrochemistry*, Plenum Press, (1997) New York.
3. E. H. Vernot, J. D. MacEwen, R. H. Bruner, C. C. Haun, E. R. Kinkead, D. E. Prentice, A. Hall III, R. E. Schmidt, R. L. Eason, G. B. Hubbard and J. T. Young, *Fundam. Appl. Toxicol.*, 5 (1985) 1050.
4. C. Wei, L. H. Yu, C. L. Cui, J. D. Lin, C. Wei, N. Mathews, F. W. Huo, T. Sritharanae and Z. C. Xu, *Chem. Commun.*, 50 (2014) 7885.
5. Y. -Y. Tang, C. -L. Kao and P. -Y. Chen, *Anal. Chim. Acta*, 711 (2012), 32.
6. M. A. Aziz and A. -N Kawde, Talanta, 115 (2013) 214.
7. S. Koçak and B. Aslışen, *Sensor. Actuat. B: Chem.*, 196 (2014) 610.
8. P. K. Rastogi, V. Ganesan and S. Krishnamoorthi, *Electrochim. Acta*, 125 (2014) 593.
9. H. L. Lin, J. M. Yang, J. Y. Liu, Y. F. Huang, J. L. Xiao and X. Zhang, *Electrochim. Acta*, 90 (2013) 382.
10. E. Ramírez-Meneses, A. M. Torres-Huerta, M. A. Domínguez-Crespo, M. G. Ponce-Varela, M. A. Hernández-Pérez, I. Betancourt and E. Palacios-González, *Electrochim. Acta*, 127 (2014) 228.
11. S. F. Lu, D. Cao, X. Xu, H. N. Wang and Y. Xiang, *RSC Adv.*, 4 (2014) 26940.
12. Y. -C. Chou, C. -Y. Tai, J. -F. Lee, T. -S. Chan and J. -M. Zen, *Electrochim. Acta*, 104 (2013) 104.
13. M. Shamsipur, Z. Karimi, M. A. Tabrizi and A. Shamsipur, *Electroanalysis*, 26 (2014) 1994.
14. G. F. Wang, C. H. Zhang, X. P. He, Z. J. Li, X. J. Zhang, L. Wang and B. Fang, *Electrochim. Acta*, 55 (2010) 7204.
15. K. N. Han, C. A. Li, M. -P. N. Bui, X. -H. Pham and G. H. Seong, *Chem. Commun.*, 47 (2011) 938.
16. Z. T. Zhao, Y. J. Sun, P. W. Li, S. B. Sang, W. D. Zhang, J. Hu and K. Lian, *J. Electrochem. Soc.*, 161 (2014) B157.
17. X. J. Zhang, A. X. Gu, G. F. Wang, W. Wang , H. Q. Wu and B. Fang, *Chem. Lett.*, 38 (2009) 466.
18. Z. J. Yin, L. P. Liu and Z. S. Yang, *J. Solid State Electrochem.*, 15 (2011) 821.
19. S. K. Mehta, K. Singh, A. Umar, G. R. Chaudhary and S. Singh, *Sci. Adv. Mater.*, 3 (2011) 962.
20. S. Babanova, U. Martinez, K. Artyushkova, K. Asazawa, H. Tanaka and P. Atanassov, *J. Electrochem. Soc.*, 161 (2014) H79.
21. F. G. Xu, Y. Liu, S. Xie and L. Wang, *Anal. Methods*, 8 (2016) 316.
22. Y. H. Wang, X. J. Yang, J. Bai, X. Jiang and G. Y. Fan, *Biosens. Bioelectron.*, 43 (2013) 180.
23. K. Ghanbari, *Synthetic Met.*, 195 (2014) 234.
24. C. Wang, L. Zhang, Z. H. Guo, J. G. Xu, H. Y. Wang, H. W. Shi, K. F. Zhai and X. Zhuo, *Electroanalysis*, 22 (2010) 1867.
25. P. Muthukumar, S. A. John, *J. Solid State Electrochem.*, 18 (2014) 2393.
26. Q. J. Wan, Y. Liu, Z. H. Wang, W. Wei, B. B. Li, J. Zou, N. J. Yang, *Electrochem. Commun.*, 29 (2013) 29.
27. C. B. Liu, H. Zhang, Y. H. Tang and S. L. Luo, *J. Mater. Chem. A*, 2 (2014) 4580.
28. C. Karuppiah, S. Palanisamy, S. -M. Chen, S. K. Ramaraj and P. Periakaruppan, *Electrochim. Acta*, 139 (2014) 157.
29. J. W. Wu, T. T. Zhou, Q. Wang and A. Umar, *Sensor. Actuat. B: Chem.*, 224 (2016) 878.
30. J. Y. Lei, X. F. Lu, W. Wang, X. J. Bian, Y. P. Xue, C. Wang and L. J. Li, *RSC Adv.*, 2 (2012) 2541.
31. M. U. A. Prathap, V. Anuraj, B. Satpati and R. Srivastava, *J. Hazard. Mater.*, 262 (2013) 766.
32. M. F. Wang, C. Wang, G. F. Wang, W. Zhang, F. Bin, *Electroanalysis*, 22 (2010) 1123.
33. F. W. Thomas Goh, Z. L. Liu, X. M. Ge, Y. Zong, G. J. Du and T. S. Andy Hor, *Electrochim. Acta*, 114 (2013) 598.

34. Z. C. Meng, Q. L. Sheng and J. B. Zheng, *J. Iran. Chem. Soc*., 9 (2012) 1007.
35. Q. G. Li, J. B. Olson and R. M. Penner, *Chem. Mater.*, 16 (2004) 3402.
36. G. C. Allen, S.J Harris, J. A. Jutson and J. M. Dyke, *Appl. Surf. Sci.*, 37 (1989) 111.
37. B. N. Ivanov-Emin, N. A. Nevskaya, B. E. Zaitsev and T. M. Ivanova, *Zh. Neorg. Khimii*, 27 (1982) 3101.
38. F. Xiao, Y. Q. Li, H. C. Gao, S. B. Ge and H. W. Duan, *Biosens. Bioelectron.*, 41 (2013) 417.
39. S. Mondal, U. Rana, R. R. Bhattacharjee and S. Malik, *RSC Adv.*, 4 (2014) 57282.
40. K. Duckers and H. P. Bonzel, *Surf. Sci.*, 213 (1989) 25.
41. Y. F. Hao, R. X. Liu, X. C. Meng, H. Y. Cheng and F. Y. Zhao, *J. Mol. Catal. A: Chem.*, 335 (2011) 183.
42. J. T. Zhang, J. W. Jiang and X. S. Zhao, *J. Phys. Chem. C*, 115 (2011) 6448.
43. B. Unnikrishnan, P. -L. Ru and S. -M. Chen, *Sensor. Actuat. B: Chem.*, 169 (2012) 235.